Nonpolar GaN films on high-index silicon: Lattice matching by design

Alex Kutana and Steven C. Erwin[*]
Center for Computational Materials Science, Naval Research Laboratory, Washington, DC 20375-5000, USA
(Received 23 July 2012; revised manuscript received 13 December 2012; published 25 January 2013)

We explore theoretically the possibility of growing GaN films in a nonpolar orientation on planar high-index Si(hhk) substrates. Candidate substrates were identified by requiring that they are well lattice matched, on a length scale of several unit cells, to GaN in the nonpolar m-plane orientation. These candidate orientations were then used to construct atomistic models of the GaN/Si(hhk) interface. Using density functional theory, we then computed the formation energies of these nonpolar interfaces and compared them to those of competing polar interfaces. We find that Si(112) and Si(113) offer potentially favorable substrates for the growth of nonpolar m-plane GaN.

DOI: 10.1103/PhysRevB.87.045314 PACS number(s): 81.15.Aa, 81.15.Hi, 68.55.−a, 81.15.Kk

I. INTRODUCTION

Gallium nitride is most often grown in wurtzite form on one of three substrates: sapphire, silicon carbide, or silicon. None of these substrates is ideally lattice matched to GaN, but high-quality films can nonetheless be grown on all three by carefully managing the strain in order to minimize dislocations. For solid-state lighting applications, sapphire and silicon carbide have long been favored because the resulting film quality is very good. But the high cost of these substrates and the difficulty of scaling up to larger wafer sizes have recently brought renewed attention to growing GaN films on silicon substrates despite the new challenges involved—for example, cracking in films thicker than 1 μm. In the last few years progress has been swift, and GaN/Si is now the basis for a rapidly expanding commercial sector; see Refs. 1 and 2 for recent reviews.

In addition to affecting the quality of the GaN film, the choice of substrate raises another important issue: its crystallographic orientation. The highest-quality GaN is obtained in the wurtzite c-plane (0001) orientation, which naturally results from growing on the (0001) surface of sapphire or silicon carbide. The same orientation is obtained by growing on the (111) surface of silicon. Because wurtzite GaN is a polar material, with spontaneous polarization along the c axis [0001], the resulting c-plane films have large internal electric fields directed normal to the film-substrate interface.[3] These fields are generally detrimental for optoelectronic applications because they reduce the overlap of electrons and holes and hence reduce the efficiency of radiative recombination.

One attractive strategy for solving this issue is to grow GaN in a nonpolar orientation, for example, in the m-plane $(1\bar{1}00)$ or a-plane $(11\bar{2}0)$ orientation; see Refs. 4 and 5 for recent reviews. This calls for a substrate that is lattice matched to both the a and c lattice parameters of GaN. Waltereit *et al.* first demonstrated the growth of high-quality nonpolar GaN using a foreign substrate, the (100) surface of γ-$LiAlO_2$, which has an atomic arrangement similar to the $(1\bar{1}00)$ surface of GaN and in-plane lattice constants within 2%.[6] The growth of nonpolar GaN has since been demonstrated on a variety of foreign substrates, including sapphire,[7,8] silicon carbide,[9] and $LiGaO_2$,[10] as well as on nonpolar surfaces of bulk GaN itself.[11,12]

Most nonpolar GaN films grown on foreign substrates show high densities of stacking faults and threading dislocations.[4] Despite these difficulties there is strong interest in combining the optoelectronic advantages of nonpolar GaN with the commercial advantages of silicon substrates. At first glance the use of silicon would appear to compound, or at least not alleviate, the problems arising from lattice mismatch because the mismatch between standard low-index silicon and nonpolar GaN is very large. In this article we explore theoretically a possible route to solving this problem: certain *high-index* silicon substrates can provide an excellent lattice match for nonpolar GaN, *provided that the Miller index is properly chosen*. To do this we use a combination of geometrical arguments and first-principles total-energy calculations, first, to identify a small set of silicon substrates, Si(hhk), that are by design well lattice matched to nonpolar GaN$(1\bar{1}00)$ and, second, to identify within this set those substrates whose predicted GaN/Si interface formation energies indicate that they are favorable for the growth of nonpolar GaN.

The remainder of this article is organized as follows. Section II provides a brief review of the current experimental status of nonpolar GaN on silicon. The central idea behind lattice matching to high-index silicon is described in Sec. III. This idea is then used in Sec. IV to identify a small set of candidate orientations Si(hhk) that are well lattice matched to nonpolar GaN. These orientations are used in Sec. V to construct GaN$(1\bar{1}00)$/Si(hhk) interface models, which are subjected to more detailed examination using density functional theory in Secs. VI and VII. The resulting best candidates are identified and their prospects are discussed in Sec. VIII.

II. CURRENT STATUS OF NONPOLAR GALLIUM NITRIDE ON SILICON

We briefly summarize below the current experimental status of nonpolar GaN grown on Si substrates. Included for completeness are results for "semipolar" GaN films, whose surface orientation is intermediate between polar (c-plane) and nonpolar (m- or a-plane) orientations. For more detailed recent reviews see Refs. 5,13, and 14.

Common to the majority of current GaN/Si growth protocols, for polar as well as semipolar and nonpolar films, is the initial deposition of an AlN buffer layer to prevent "melt-back etching" of Si by Ga.[15–17] Because of the need for this buffer

layer, our theoretical treatment will also consider AlN/Si lattice matching and interface formation energies.

A. Low-index silicon substrates

By far the most commonly used silicon substrate for GaN growth is Si(111). On this substrate, GaN invariably grows in the polar *c*-plane orientation, presumably due to the threefold symmetry of unreconstructed Si(111). The other two low-index silicon orientations, Si(110) and Si(001), have been much less investigated as substrates for GaN. The Si(110) surface, interestingly, offers an excellent lattice match (in one direction) for AlN buffer layers grown in the polar *c*-plane orientation.[18] This leads to high-quality *c*-plane films free of cracks[19] but probably preempts the possibility of semipolar or nonpolar GaN films on Si(110) substrates.

For Si(001) substrates, Schulze *et al.* have shown that semipolar *r*-plane GaN($1\bar{1}02$) can be grown by inserting low-temperature AlN interlayers into the buffer layer.[20,21] One complication is that the fourfold symmetry of unreconstructed Si(001) leads to four equivalent in-plane alignments of the GaN *r*-plane rectangular unit cell. (The $2 \times 1/1 \times 2$ reconstruction of Si(001) still leaves two equivalent alignments.) One of these can be preferentially selected by miscutting the silicon a few degrees away from (001),[20] but the resulting films are nonetheless rough and unsuitable for device applications.[18]

B. Patterned silicon substrates

Honda *et al.* first demonstrated that by chemically etching a Si(001) substrate to expose tilted Si(111) facets and then growing GaN in the standard polar *c*-plane orientation on these facets (using a mask for selective area growth), the resulting film had, by virtue of the tilt, a semipolar ($1\bar{1}01$) orientation.[22] Since then, this approach has also been used to grow semipolar GaN($11\bar{2}2$) on patterned Si(113),[23] nonpolar *a*-plane GaN($11\bar{2}0$) on patterned Si(110),[24,25] and nonpolar *m*-plane GaN($1\bar{1}00$) on patterned Si(112).[26,27]

An important aspect of this patterned growth method is that the individual GaN crystallites grown on each facet must eventually be coalesced. Achieving a smooth, continuous film using this epitaxial lateral overgrowth (ELO) approach requires slower growth rates.

C. High-index silicon substrates

Investigations of nonpatterned, high-index silicon as a substrate for GaN growth are quite new. Ravash *et al.*[28] prepared a hydrogen-terminated Si(112) surface, then deposited a monolayer of Al, the AlN buffer layer, and several GaN/AlN interlayers. When GaN was grown on this substrate, it was found that the *c* axis was inclined by $\sim 18^\circ$ from the substrate surface normal. This is close to the angle (19.5°) between the (111) and (112) planes, suggesting that the film grew in the standard *c*-plane orientation on (111) terraces of the Si(112) surface. This outcome is sensible in light of the known structure of clean Si(112): a sawtooth consisting of alternating (111) and (337) facets.[29]

Subsequent experiments confirmed this interpretation by growing GaN on the substrate series Si(112), Si(113), Si(114), Si(115), Si(116).[30–32] Across this series the observed tilt of the GaN *c* axis increased monotonically and in reasonable quantitative agreement with the angles of the crystal planes relative to (111). Hence these GaN/Si(11*k*) films all had semipolar orientations with inclination angles depending on *k*. Further efforts toward optimization showed that by using a high-temperature AlN seed layer, smooth and continuous semipolar GaN films could be grown on Si(11*k*).[19] Thus the use of high-index silicon substrates accomplished, on a much smaller length scale, a goal conceptually similar to that of patterned substrates.

These experimental results—polar growth on (111) terraces, leading to semipolar GaN films—are not the only possible outcome for GaN grown on high-index Si(*hhk*). It is known from scanning tunneling microscopy studies that there are three silicon surfaces oriented between (001) and (111) with stable, planar reconstructions: Si(113), Si(114), and Si(5,5,12).[33] Between (111) and (110) there is another, Si(331).[34] Structural models for these surfaces do not have (111) terraces.[34–40] Hence it is unclear whether substrates with these stable orientations necessarily lead to semipolar GaN with the *c* axis tilted according to the index. In the remainder of this article we investigate possible alternatives to this outcome.

III. LATTICE MATCHING WITH HIGH-INDEX SILICON

In order to obtain a completely nonpolar GaN film, the *c* axis must be parallel to the surface plane of the film. For growth on a planar substrate this means the *c* axis must lie in the surface plane of the substrate as well. This is unlikely to occur on Si(111) or Si(001) because of the very large mismatch between the GaN and Si lattice parameters.

Here we explore theoretically the possibility of growing completely nonpolar GaN films using a high-index Si surface as the substrate. The central idea is to identify a Si substrate plane, (*hhk*), that satisfies two requirements: (1) The Si(*hhk*) substrate should be well lattice matched, *on the length scale of a few GaN unit cells,* to GaN in a nonpolar orientation. (2) The interface between Si(*hhk*) and the nonpolar GaN should have a lower formation energy than that of competing polar interfaces such as GaN(0001)/Si(111).

The first of these requirements can be satisfied by searching, within the large space of Si(*hhk*) crystal planes, for two-dimensional coincidence-site lattices (CSLs) common to both Si and GaN, that is, planar Bravais lattices whose dimensions are small integer multiples of both the Si(*hhk*) and GaN unit-cell dimensions. An exact multiple is neither plausible nor required; we search for short-period CSLs that nonetheless lead to small GaN strain (less than, say, 3%). To satisfy the second requirement we use density functional theory to evaluate the formation energies of a few candidate films that satisfy the CSL matching criterion. By comparing the formation energies of these nonpolar GaN/Si films to those of polar GaN(0001)/Si(111) films, one can, in principle, predict whether this polar growth mode is likely to preempt the nonpolar modes. To keep the scope of the study reasonable, we will consider nonpolar GaN only in the *m*-plane ($1\bar{1}00$) orientation.

Despite its simplicity, we believe such an approach is promising because it has already been shown to work in the reverse sense by successfully predicting the crystallographic

orientation of a strongly lattice-mismatched film grown on m-plane GaN. Reference 41 reports the experimental growth by molecular-beam epitaxy of Fe on m-plane GaN, together with a theoretical analysis of the Fe/GaN film. Despite different crystal structures and strongly mismatched lattice constants, the resulting Fe films were observed to be single crystal, with a high Miller index and a unique orientational relationship to the GaN substrate. To analyze these films theoretically, the two requirements described above were applied. First, a geometrical search was performed in the space of Fe($h0\ell$) orientations for CSLs with both small strain and small CSL period. This search led to a small set of plausible candidates: (207), (205), (203), plus their reflected counterparts ($h0\bar{\ell}$). Density functional theory (DFT) calculations of the Fe/GaN interface formation energies of these six candidates identified Fe(205) as the most favorable. This prediction of Fe(205)/GaN($1\bar{1}00$) as the preferred film orientation was then confirmed experimentally using convergent-beam electron diffraction.

For the growth of GaN on silicon there is an additional practical consideration that must be considered: preventing the melt-back etching of Si by Ga during the initial stage of growth. As described in Sec. II this can be done by first depositing a buffer layer of AlN. For this reason, the choice of the most promising Si(hhk) substrates for GaN growth may depend in part, or even primarily, on the stability of an AlN buffer film on the Si substrate. Therefore we consider here nonpolar films of both GaN($1\bar{1}00$) and AlN($1\bar{1}00$) on Si(hhk). From a practical standpoint, if a high-quality nonpolar AlN buffer layer can be grown on Si(hhk), then the subsequent growth of nonpolar GaN would likely succeed because of its close lattice match and chemical compatibility with AlN.

IV. COINCIDENCE SITE LATTICES

We begin the search for candidate Si(hhk) substrates by constructing CSLs common to Si and Ga. The Si(hhk) surface can be obtained by cutting the Si(001) surface at an angle given by $\tan(\theta) = \sqrt{2}h/k$, creating a surface plane whose normal is tilted with respect to the [001] direction. Figure 1 shows schematically the example of the Si(112) surface. Along the x axis of Fig. 1, the Si(hhk) unit cell has length $a_s(h^2 + k^2/2)^{1/2}$, where $a_s = 5.47$ Å is the theoretical (DFT) lattice constant of silicon; for Si(112) this period is $\sqrt{3}a_s$. Into the plane of Fig. 1 (the y axis) the length of the unit cell is $2 \times a_s/\sqrt{2}$ for any (hhk). The factor 2 arises from using a doubled primitive cell to permit dimerization of the silicon surface in cases where this is energetically favorable.

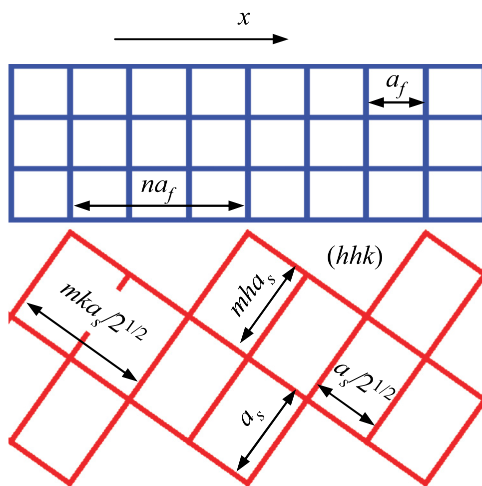

FIG. 1. (Color online) Coincidence lattice between Si(112) surface (bottom) and m-plane wurtzite GaN (or AlN) film (top).

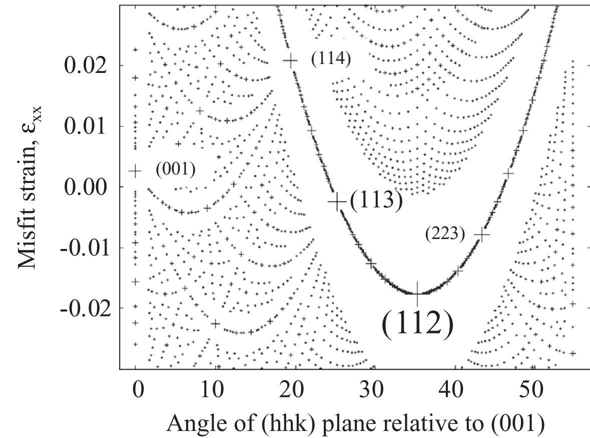

FIG. 2. Misfit strain in the m-plane wurtzite GaN film forming commensurate interfaces with Si(hhk) substrates. The points represent all possible Si(hhk) planes having $h \leqslant k \leqslant 50$. The misfit ε_{xx} is the strain component along the [$11\bar{2}0$] direction of the GaN film. The size of the symbols is proportional to $1/n$, where n is the number of GaN unit cells in the CSL. Si(hhk) planes for which GaN films have both small misfit strain and small CSL period are labeled.

The condition for exact commensurability between the m-plane GaN film and Si(hhk) substrate in the x direction is $na_f = ma_s(h^2 + k^2/2)^{1/2}$, where a_f is the lattice constant of the film in that direction. The relevant value of a_f depends on the orientation of the rectangular surface unit cell of the m-plane GaN with respect to the Si substrate. There are two plausible choices. In the first orientation, the GaN c axis is along y, so that $a_f = a$, whereas in the second orientation the c axis is along x, so that $a_f = c$. Here, $a = 3.22$ Å and $c = 5.25$ Å are the DFT lattice parameters of wurtzite GaN. For all (hhk) we assumed the first of these orientations because a small 3(GaN) : 2(Si) CSL along the y direction reduces the misfit strain in this direction to a reasonably low value, $\varepsilon_{yy} = -1.8\%$. The same 3 : 2 CSL also works well for AlN, for which the corresponding misfit strain is 2.9%. The second orientation requires a much larger CSL of 12 : 5 to keep the strain below 3%. This latter period is almost certainly too large to be physically realistic, and so this orientation was not considered further.

Having fixed the orientation of the GaN film, we now turn to the task of finding candidate CSLs with small period and small strain along the x direction. Figure 2 shows the CSL period and misfit strain and for crystal planes (hhk) between (001) and (111). To make the visual identification of planes with short CSL periods easy, the size of the plot symbol was made proportional to $1/n$, where n is the number of GaN unit cells in the CSL. There are five orientations having both small strain and short coincidence periods: (001), (112), (113), (114), and (223). These are the candidate orientations we used

as the starting point for DFT calculations of GaN/Si and AlN/Si formation energies, which are described next.

V. INTERFACE STRUCTURES

We modeled epitaxial films of GaN and AlN using stoichiometric slabs with four to six atomic layers, with the topmost layer having 1×1 periodicity prior to structural relaxation. For c-plane films, both Ga-polar and N-polar orientations were treated. The Si(hhk) substrates were represented by slabs with a similar number of layers, passivated on the bottom with hydrogen. All GaN and Si atomic positions were fully relaxed except the bottom Si layer. Total energies and forces were calculated within the Perdew-Burke-Ernzerhof (PBE) generalized-gradient approximation[42] to DFT using projector-augmented-wave (PAW) potentials as implemented in VASP.[43] The plane-wave cutoff for all calculations was 400 eV.

For each film orientation the formation energy depends strongly on the choice of GaN-Si interface registry. We systematically varied the registry over a grid in both x and y to locate the global energy minimum for each orientation.

Figure 3 shows the resulting equilibrium structures of nonpolar GaN films on Si(112) and Si(113) substrates. These two interfaces have a distinct feature—a favorable alignment of atoms across the interface plane—not shared by the other candidate orientations. This suggests that Si(112) and Si(113) may be unusually well suited for the growth of nonpolar GaN (and AlN). In the next section we will establish this quantitatively using the DFT formation energies of the films.

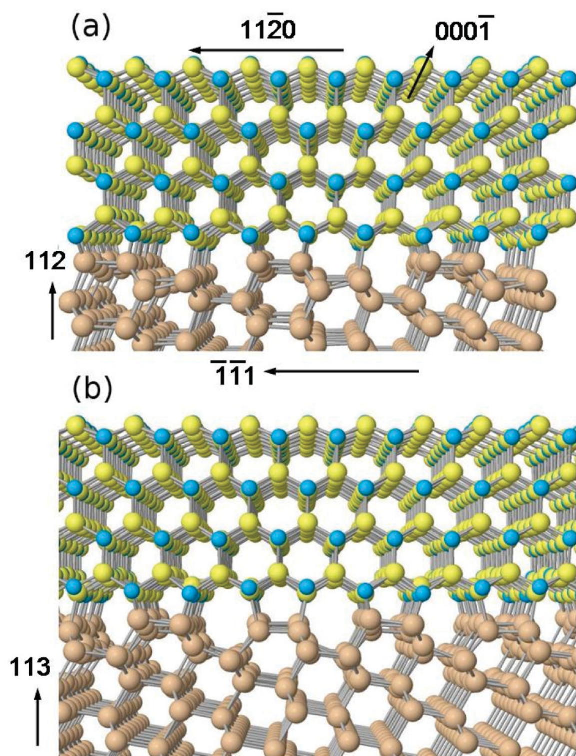

FIG. 3. (Color online) Relaxed nonpolar GaN films on lattice-matched high-index silicon substrates. (a) GaN/Si(112). (b) GaN/Si(113). Gallium atoms are yellow (lightest circles), nitrogen atoms are blue (darkest circles), and silicon atoms are brown.

Before doing so, however, it is helpful to gain insight by examining the interfaces in Fig. 3 in more detail. It is clear from visual inspection that, in both orientations, the rows of atoms along the c axis are able to form a one-to-one correspondence across the interface. Interfacial Si atoms have either one or two dangling bonds. We find here that most Si atoms with two dangling bonds (usually) form two bonds, to two atoms, across the interface; most of the single dangling bonds correctly form one interface bond. As a result only very few Si atoms are undercoordinated. In contrast, on Si(001), Si(114), and Si(223) this one-to-one matching cannot occur, and the number of undercoordinated atoms is significantly larger.

VI. FORMATION ENERGY FORMALISM

The formation energy E_f of a GaN film on a Si substrate is defined as

$$E_f = E_t - n_{\rm Si}\,\mu_{\rm Si} - n_{\rm Ga}\,\mu_{\rm Ga} - n_{\rm N}\,\mu_{\rm N}, \qquad (1)$$

where E_t is the total energy of the computational unit cell containing $n_{\rm Si}$ atoms of Si, $n_{\rm Ga}$ atoms of Ga, and $n_{\rm N}$ atoms of N. Thermodynamic equilibrium with both Si and (unstrained) GaN implies that the atomic chemical potentials obey the constraints $\mu_{\rm Si} = E_t^{\rm Si}$ (the energy per atom in bulk Si) and $\mu_{\rm Ga} + \mu_{\rm N} = E_t^{\rm GaN}$ (the energy per formula unit in bulk GaN). For stoichiometric films we have $n_{\rm Ga} = n_{\rm N}$, and therefore E_f is independent of the Ga (and N) chemical potential.

Two important physical effects motivate us to modify and extend the formation energies given by Eq. (1). The first effect arises from the small residual strain in the GaN due to the CSL. The consequence of this strain is an additional energy penalty that eventually, for thick films, dominates the formation energy and becomes linear in the film thickness. Although this effect is important for thick films (for example, it leads to misfit dislocations for films beyond their critical thickness[44]), it is not relevant for the very early stage of growth we study here. A more relevant measure is the formation energy of the fully strain-relaxed GaN film, which is independent of film thickness. In the hypothetical case where the CSL strain is exactly zero, this film formation energy is exactly given by E_f. Following this line of reasoning, we define an "unstrained formation energy" E_f^0 by subtracting from E_f the thickness-dependent contribution due to the CSL strain. In the tables and discussion below we report these unstrained formation energies E_f^0.

We evaluated the CSL strain-energy contributions using the known strains together with bulk elastic constants. For the m-plane film orientations used in this work, the elastic energy per unit volume is

$$U = \tfrac{1}{2}C_{11}\varepsilon_{xx}^2 + \tfrac{1}{2}C_{33}\varepsilon_{yy}^2 + C_{13}\varepsilon_{xx}\varepsilon_{yy}, \qquad (2)$$

where ε_{xx} and ε_{yy} are the corresponding deformations of the film along the $[11\bar{2}0]$ and [0001] axes and C_{11} and C_{33} are the elastic constants of the wurtzite GaN or AlN. For the c-plane orientation, the elastic energy contribution reads

$$U = \tfrac{1}{2}C_{11}\left(\varepsilon_{xx}^2 + \varepsilon_{yy}^2\right) + C_{12}\varepsilon_{xx}\varepsilon_{yy}. \qquad (3)$$

TABLE I. Calculated formation energies (meV/Å^2) of the ideal relaxed stoichiometric m-plane GaN and AlN thin films on various Si(hhk) surfaces. The film-thickness-dependent contribution from the bulk stress is not included in these values and needs to be added when evaluating the total formation energy of the films with finite thickness.

Si surface	GaN	AlN
(001)	201	250
(112)	182	234
(113)	178	231
(114)	193	225
(223)	196	252

Here, ε_{xx} and ε_{yy} are the deformations along the $[11\bar{2}0]$ and $[1\bar{1}00]$ axes. When calculating the contributions from Eqs. (2) and (3), either the theoretical[45] or experimental[46–48] values of elastic constants of GaN and AlN can be used; we used theoretical values from Ref. 45.

VII. FORMATION ENERGY RESULTS

Table I lists the resulting formation energies of nonpolar stoichiometric m-plane GaN and AlN films on the five Si(hhk) surfaces identified in Sec. IV. Nonpolar GaN films have the lowest formation energy on the Si(113) substrate, followed by Si(112). For nonpolar AlN, the lowest-energy substrate is Si(114), followed by Si(113) and Si(112). It is noteworthy that these high-index Si substrates lead to substantially lower formation energies, for both GaN and AlN, than the low-index Si(001) does.

The energies of these nonpolar films are compared with those of polar c-plane films in Tables II and III. The energies of c-plane films were calculated only on those Si(hhk) surfaces where commensurate lattices with small CSL periods could be found; the formation energies of c-plane films on Si(111) are also given. It is evident from Tables II and III that the lowest formation energies are obtained for the ideal nonpolar surfaces of both GaN and AlN. For GaN the ideal polar (0001) and $(000\bar{1})$ orientations have much higher energy than the nonpolar m plane. For AlN the ideal $(000\bar{1})$ film is still higher in energy but is comparable with the nonpolar case, whereas the (0001) film is significantly higher in energy than the nonpolar film.

The second important physical effect we must address is that the experimentally realized free surfaces of the films may differ from the ideal (1×1 stoichiometric) surfaces we have assumed. In general, the stable surface reconstruction and stoichiometry depend on the experimental chemical potential conditions describing the growth.[49–55] To properly take into account this dependence requires that we extend our

TABLE II. Calculated formation energies (meV/Å^2) of the ideal relaxed stoichiometric GaN thin films on various Si(hhk) surfaces.

Si surface	GaN$(1\bar{1}00)$	GaN(0001)	GaN$(000\bar{1})$
(112)	182	244	310
(113)	178	222	319
(111)		219	303

TABLE III. Calculated formation energies (meV/Å^2) of the ideal relaxed stoichiometric AlN thin films on various Si(hhk) surfaces.

Si surface	AlN$(1\bar{1}00)$	AlN(0001)	AlN$(000\bar{1})$
(112)	234	266	239
(113)	231	291	245
(111)		299	262

calculated formation energies to allow for nonstoichiometric, and possibly reconstructed, free surfaces.

These extensions are more important for c-plane films than m-plane films, where the 1×1 stoichiometric Ga-N (Ref. 52) and Al-N (Ref. 55) surface-dimer terminations are stable over a wide range of chemical potentials. Only in highly Ga-rich (or Al-rich) conditions do other m-plane terminations, such as "Ga adatom on Ga monolayer" or "Ga bilayer on Ga dimers" (Ref. 52) or "2Al" (Ref. 55), become energetically preferable to the ideal 1×1 stoichiometry. In contrast, for c-plane films the ideal stoichiometric termination is never preferred. Thus it is particularly important to extend our results for stoichiometric polar films. We made these corrections by combining the stoichiometric formation energies in Tables I–III with the appropriate energy differences obtained by other authors, using similar methodology, for the various reconstructions of polar GaN (Ref. 52) and AlN (Ref. 55).

The four panels of Fig. 4 display our resulting formation energies for reconstructed GaN and AlN films on Si(112) and (113) as a function of chemical potential. For GaN we find that the stoichiometric nonpolar m-plane film is indeed energetically preferred to c-plane films of either polarity, over a wide range of Ga chemical potential, on both Si(112) and Si(113) substrates. This result is tantalizing in principle but will be problematic to realize in practice because of the experimental difficulty of growing GaN directly on silicon. Hence we turn to the results for AlN on Si(112) and Si(113). Here we find, unfortunately, that the nonpolar film is *not* energetically favored for any value of Al chemical potential on either substrate. Instead, on both substrates a N-polar $(000\bar{1})$ film, with one of two Al-rich reconstructions, is favored. The reason underlying this strong preference for N polarity can be ultimately traced back to the large stabilization energy of the Al-rich N-polar c plane of AlN.[55]

VIII. DISCUSSION AND CONCLUSIONS

It is important to acknowledge the limited scope of this initial study. Two assumptions, made here primarily for computational convenience, deserve close attention in future work. The first assumption is that the terminating interfacial layer of GaN and AlN films is a simple stoichiometric termination of the bulk phase. While this may be reasonable, it is also possible that more realistic interface geometries exist. Exploration of this possibility is an important task for future work.

The second assumption concerns the initial state of the silicon substrate, which was taken to be dimerized prior to formation of the interface and subsequent relaxation. In reality, the initial substrate structure depends on the conditions at the beginning of the film growth.

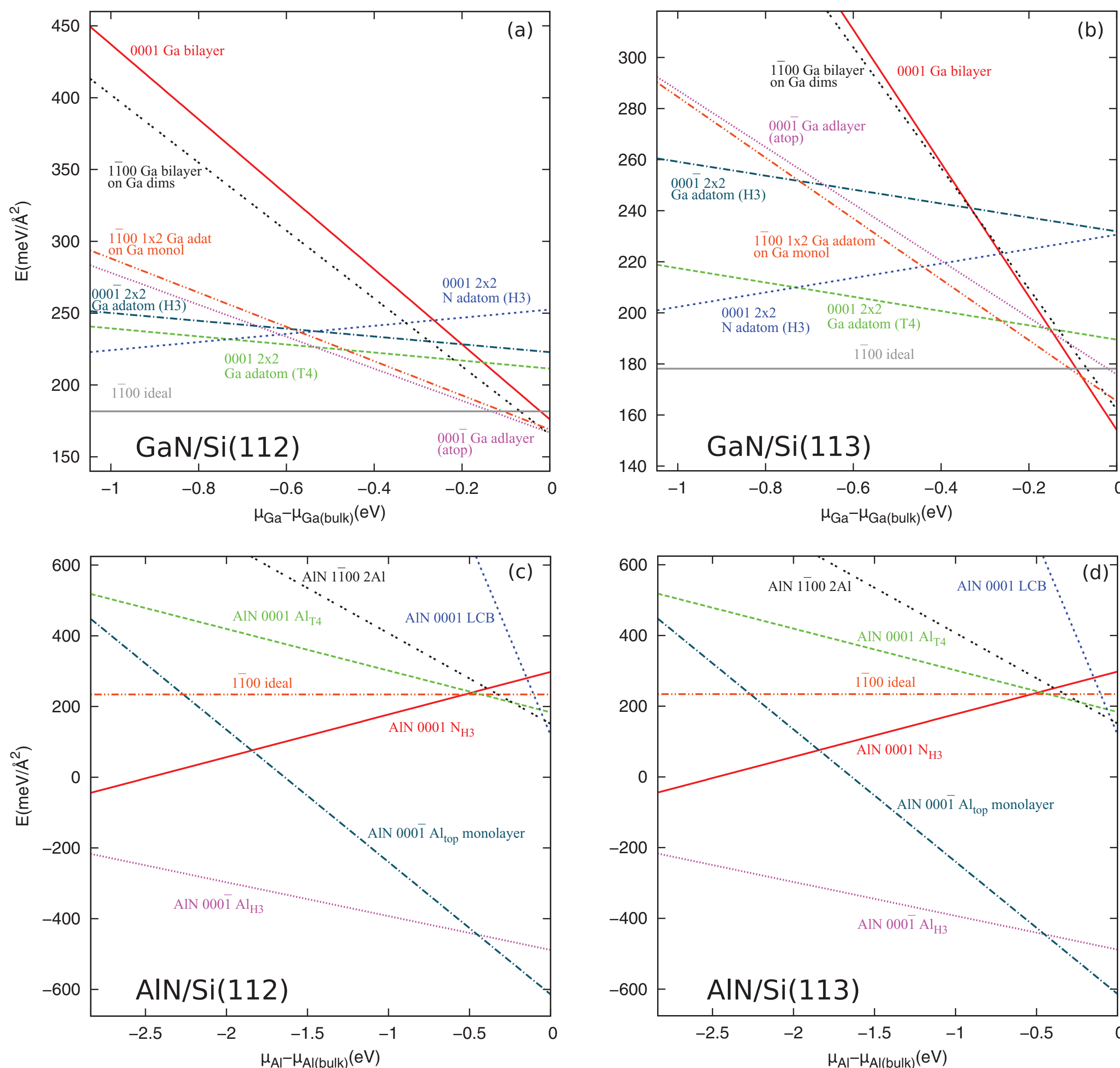

FIG. 4. (Color online) Formation energies of (a) GaN films on Si(112), (b) GaN films on Si(113), (c) AlN films on Si(112), and (d) AlN films on Si(113). These energies are based on the stoichiometric formation energies in Tables I–III supplemented by theoretical results in Refs. 52 and 55. Labels are taken from those publications.

In general, arbitrary clean Si(*hhk*) surfaces do not exist, as they prefer to form low-index facets, such as (001) and (111) in their lowest-energy state. As discussed in Sec. II, there are three Si(*hhk*) surfaces between Si(001) and Si(111), i.e., Si(113), Si(114), and Si(5,5,12), with stable, planar reconstructions.[33] In particular, we note that Si(113) forms stable 3×2 planes at room temperature.[33,35] In addition, faceted clean Si(112) (Ref. 29) becomes planarized after the adsorption of Ga (Ref. 56) or Al.[57]

It is remarkable that the two Si surfaces that are predicted here to be the best candidates for direct growth of nonpolar GaN, namely, Si(113) and Si(112), are stable or can be stabilized prior to growing GaN. Here, we did not employ the 3×2 reconstructed Si(113) surface as a starting structure due to the low-period CSL requirements. Likewise, no attempts at starting with a Ga-seeded Si(112) surface have been made, as the conditions that favor nonpolar GaN growth are nitrogen rich. Nevertheless, we suggest that these two orientations may deserve experimental scrutiny as potential silicon substrates for nonpolar GaN growth.

In highly nitrogen-rich conditions, nitridation of the silicon surface may occur before the formation of the GaN film. It is clear that nitridation should be avoided in order to achieve a direct interface that promotes nonpolar growth, but the feasibility of such a pathway was not addressed here. As the results in Figs. 4(a) and 4(b) show, stabilizing the nonpolar GaN film requires conditions that are at least moderately nitrogen rich, a requirement that competes with the requirement of preventing surface nitridation. The difficulty of satisfying both of these requirements may be part of the reason for earlier failures in growing nonpolar GaN films on silicon. We hope that our work will stimulate more theoretical and

experimental effort in this area that will help answer some of these questions.

In summary, we performed a theoretical and computational study of the feasibility of growing nonpolar GaN or AlN films on high-index Si(hhk) substrates. By requiring that the substrate satisfies two requirements, a lattice-matching condition within a modest coincidence-site lattice and a low interface formation energy within density functional theory, we have demonstrated that it may be possible to grow nonpolar m-plane GaN on Si(112) and Si(113) under mildly nitrogen-rich conditions.

ACKNOWLEDGMENTS

The authors thank Sergio Fernandez-Garrido for helpful and stimulating discussions and Noam Bernstein and Stephen Hellberg for a critical reading of the manuscript. This work was supported by the Office of Naval Research and the ASEE program at NRL. Computations were performed at the DoD Major Shared Resource Center at AFRL and at the DoD HPCMP Open Research Systems.

APPENDIX: EVALUATION OF THE THERMODYNAMIC STABILITY OF THE INTERFACE

The general procedure for computing the Gibbs free energy of formation of a compound such as a molecule or solid involves evaluating its stability in relation to the constituent atomic species in their standard states. When the number of atoms in the system is varied, the Gibbs free energy of formation will depend on the chemical potential of the atomic species. The specific procedure for surfaces and interfaces is outlined in Refs. 58 and 59; its main steps will be repeated here for convenience.

The surface is assumed to be near thermodynamic equilibrium with the bulk phase, so that the chemical potential of a given species of atoms on the surface is same as in the bulk. The Gibbs free energy of the surface g_S is defined as an additional free energy that is required to form a unit area of the surface from the bulk, according to the following formula:

$$g_S A = G_{\mathrm{sys}} - G_0. \tag{A1}$$

Here, G_{sys} is the actual calculated total free energy of the model slab representing the surface, A is the surface area of the model slab, and G_0 is the free energy of the hypothetical bulk structure with the same number of atoms. The free energy G_{sys} may include a contribution from the lateral stress if the lattice constants of the film and substrate do not match perfectly. The Gibbs free energy G_0 can be written in terms of chemical potentials and numbers of atoms as follows:

$$G_0 = \sum_{i=1}^{n} \mu_i N_i. \tag{A2}$$

Here, μ_i is the chemical potential of the ith component in the bulk, N_i is the number of atoms in the ith component, and n is the total number of components in the system. In addition, at constant pressure and temperature, which is an assumption about the external conditions that was made throughout this work, the Gibbs-Duhem equation is satisfied:

$$\sum_{i=1}^{n} N_i d\mu_i = 0. \tag{A3}$$

After integrating Eq. (A3) at fixed N_i, one obtains

$$\sum_{i=1}^{n} N_i \mu_i = \mathrm{const}; \tag{A4}$$

that is, out of n chemical potentials only $n-1$ can be varied independently.

In a multicomponent alloy, there exist limits on the ranges of variations of independent μ_i, imposed by the requirement of chemical stability of the alloy with respect to decomposition into single-component phases. For instance, in bulk GaN, the chemical potential of Ga atoms cannot exceed that of the bulk Ga, or all Ga atoms would leave the GaN phase and coalesce into the Ga crystal. Likewise, the chemical potential of nitrogen atoms in GaN cannot exceed that of the N atoms in the N_2 gas. Writing these stability conditions as

$$\mu_{\mathrm{Ga}} \leqslant \mu_{\mathrm{Ga(bulk)}}, \tag{A5}$$

$$\mu_{\mathrm{N}} \leqslant \mu_{\mathrm{N(gas)}} \tag{A6}$$

and combining them with Eq. (A4), the following limiting equations for the values of chemical potentials of the components are obtained:

$$(G_0 - N_N \mu_{\mathrm{N(gas)}})/N_{\mathrm{Ga}} \leqslant \mu_{\mathrm{Ga}} \leqslant \mu_{\mathrm{Ga(bulk)}}, \tag{A7}$$

$$(G_0 - N_{\mathrm{Ga}} \mu_{\mathrm{Ga(bulk)}})/N_{\mathrm{N}} \leqslant \mu_{\mathrm{N}} \leqslant \mu_{\mathrm{N(gas)}}. \tag{A8}$$

By introducing the standard enthalpy of formation of GaN, $\Delta_f H^{\mathrm{o}}_{\mathrm{GaN(bulk)}} = \mu_{\mathrm{GaN(bulk)}} - \mu_{\mathrm{Ga(bulk)}} - \mu_{\mathrm{N(gas)}}$, Eqs. (A7) and (A8) can also be written as

$$\mu_{\mathrm{Ga(bulk)}} + \Delta_f H^{\mathrm{o}}_{\mathrm{GaN(bulk)}} \leqslant \mu_{\mathrm{Ga}} \leqslant \mu_{\mathrm{Ga(bulk)}}, \tag{A9}$$

$$\mu_{\mathrm{N(gas)}} + \Delta_f H^{\mathrm{o}}_{\mathrm{GaN(bulk)}} \leqslant \mu_{\mathrm{N}} \leqslant \mu_{\mathrm{N(gas)}}. \tag{A10}$$

In the general case of an arbitrary number of components, the restrictions on the values of the chemical potentials are imposed based on the requirement of stability with respect to decomposition into one-component, two-component, three-component, etc., compounds:

$$\begin{gathered} \mu_i \leqslant \mu_{i(\mathrm{bulk})}, \\ \mu_i + \mu_j \leqslant \mu_{ij(\mathrm{bulk})}, \\ \mu_i + \mu_j + \mu_k \leqslant \mu_{ijk(\mathrm{bulk})}, \\ \cdots \end{gathered} \tag{A11}$$

Just as in the case of a two-component mixture, these equations allow one to determine the allowed ranges of the values of the chemical potentials in a multicomponent mixture.

*steve.erwin@nrl.navy.mil

[1] *III-V Compound Semiconductors: Integration with Silicon-Based Microelectronics*, edited by T. Li, M. Mastro, and A. Dadgar (CRC Press, Boca Raton, FL, 2010).

[2] A. Dadgar, T. Hempel, J. Blaesing, O. Schulz, S. Fritze, J. Christen, and A. Krost, Phys. Status Solidi C **8**, 1503 (2011).

[3] T. Takeuchi, S. Sota, M. Katsuragawa, M. Komori, H. Takeuchi, H. Amano, and I. Akasaki, Jpn. J. Appl. Phys. **36**, L382 (1997).

[4] J. S. Speck and S. F. Chichibu, MRS Bull. **34**, 304 (2009).

[5] F. Scholz, Semicond. Sci. Technol. **27**, 024002 (2012).

[6] P. Waltereit, O. Brandt, A. Trampert, H. T. Grahn, J. Menniger, M. Ramsteiner, M. Reiche, and K. H. Ploog, Nature (London) **406**, 865 (2000).

[7] M. D. Craven, S. H. Lim, F. Wu, J. S. Speck, and S. P. DenBaars, Appl. Phys. Lett. **81**, 469 (2002).

[8] H. M. Ng, Appl. Phys. Lett. **80**, 4369 (2002).

[9] M. D. Craven, F. Wu, A. Chakraborty, B. Imer, U. K. Mishra, S. P. DenBaars, and J. S. Speck, Appl. Phys. Lett. **84**, 1281 (2004).

[10] M. M. C. Chou, C. Chen, D. R. Hang, and W.-T. Yang, Thin Solid Films **519**, 5066 (2011).

[11] T. Detchprohm, M. Zhu, Y. Li, Y. Xia, C. Wetzel, E. A. Preble, L. Liu, T. Paskova, and D. Hanser, Appl. Phys. Lett. **92**, 241109 (2008).

[12] Y. Yoshizumi, M. Adachi, Y. Enya, T. Kyono, S. Tokuyama, T. Sumitomo, K. Akita, T. Ikegami, M. Ueno, K. Katayama, and T. Nakamura, Appl. Phys. Express **2**, 092101 (2009).

[13] S. A. Kukushkin, A. V. Osipov, V. N. Bessolov, B. K. Medvedev, V. K. Nevolin, and K. A. Tcarik, Rev. Adv. Mater. Sci. **17**, 1 (2008).

[14] Q. Sun and J. Han, *GaN and ZnO-Based Materials and Devices* (Springer, Berlin, 2012), Chap. 1, pp. 1–27.

[15] H. Ishikawa, K. Yamamoto, T. Egawa, T. Soga, T. Jimbo, and M. Umeno, J. Cryst. Growth **189**, 178 (1998).

[16] R. Ravash, J. Blaesing, T. Hempel, M. Noltemeyer, A. Dadgar, J. Christen, and A. Krost, Phys. Status Solidi B **248**, 594 (2011).

[17] A. Dadgar, R. Ravash, P. Veit, G. Schmidt, M. Müller, A. Dempewolf, F. Bertram, M. Wieneke, J. Christen, and A. Krost, Appl. Phys. Lett. **99**, 021905 (2011).

[18] A. Dadgar, F. Schulze, M. Wienecke, A. Gadanecz, J. Blasing, P. Veit, T. Hempel, A. Diez, J. Christen, and A. Krost, New J. Phys. **9**, 389 (2007).

[19] F. Reiher, A. Dadgar, J. Bläsing, M. Wieneke, and A. Krost, J. Cryst. Growth **312**, 180 (2010).

[20] F. Schulze, A. Dadgar, J. Bläsing, and A. Krost, Appl. Phys. Lett. **84**, 4747 (2004).

[21] F. Schulze, A. Dadgar, J. Blasing, and A. Krost, J. Cryst. Growth **272**, 496 (2004).

[22] Y. Honda, N. Kameshiro, M. Yamaguchi, and N. Sawaki, J. Cryst. Growth **242**, 82 (2002).

[23] M. Yang, H. S. Ahn, T. Tanikawa, Y. Honda, M. Yamaguchi, and N. Sawaki, J. Cryst. Growth **311**, 2914 (2009).

[24] T. Tanikawa, D. Rudolph, T. Hikosaka, Y. Honda, M. Yamaguchi, and N. Sawaki, J. Cryst. Growth **310**, 4999 (2008).

[25] N. Sawaki, T. Hikosaka, N. Koide, S. Tanaka, Y. Honda, and M. Yamaguchi, J. Cryst. Growth **311**, 2867 (2009).

[26] X. Ni, M. Wu, J. Lee, X. Li, A. A. Baski, U. Özgür, and H. Morkoç, Appl. Phys. Lett. **95**, 111102 (2009).

[27] N. Izyumskaya, S. Liu, V. Avrutin, X. Ni, M. Wu, U. Ozgur, S. Metzner, F. Bertram, J. Christen, and L. Zhou, J. Cryst. Growth **314**, 129 (2011).

[28] R. Ravash, J. Bläsing, T. Hempel, M. Noltemeyer, A. Dadgar, J. Christen, and A. Krost, Appl. Phys. Lett. **95**, 242101 (2009).

[29] A. A. Baski and L. J. Whitman, Phys. Rev. Lett. **74**, 956 (1995).

[30] R. Ravash, J. Blaesing, A. Dadgar, and A. Krost, Appl. Phys. Lett. **97**, 142102 (2010).

[31] R. Ravash, P. Veit, M. Müller, G. Schmidt, A. Dempewolf, T. Hempel, J. Bläsing, F. Bertram, A. Dadgar, J. Christen, and A. Krost, Phys. Status Solidi C **9**, 507 (2012).

[32] R. Ravash, A. Dadgar, F. Bertram, A. Dempewolf, S. Metzner, T. Hempel, J. Christen, and A. Krost, J. Cryst. Growth (2012), doi:10.1016/j.jcrysgro.2012.08.033.

[33] A. A. Baski, S. C. Erwin, and L. J. Whitman, Surf. Sci. **392**, 69 (1997).

[34] C. Battaglia, K. Gaal-Nagy, C. Monney, C. Didiot, E. F. Schwier, M. G. Garnier, G. Onida, and P. Aebi, Phys. Rev. Lett. **102**, 066102 (2009).

[35] J. Dąbrowski, H.-J. Müssig, and G. Wolff, J. Vac. Sci. Technol. B **13**, 1597 (1995).

[36] S. C. Erwin, A. A. Baski, and L. J. Whitman, Phys. Rev. Lett. **77**, 687 (1996).

[37] A. A. Baski, S. C. Erwin, and L. J. Whitman, Science **269**, 1556 (1995).

[38] F. C. Chuang, C. V. Ciobanu, C. Predescu, C. Z. Wang, and K. M. Ho, Surf. Sci. **578**, 183 (2005).

[39] H. D. Kim, H. T. Li, Y. Z. Zhu, J. R. Hahn, and J. M. Seo, Surf. Sci. **601**, 1831 (2007).

[40] H. Kim, H. Li, and J. M. Seo, J. Vac. Sci. Technol. B **25**, 1511 (2007).

[41] S. C. Erwin, C. X. Gao, C. Roder, J. Lähnemann, and O. Brandt, Phys. Rev. Lett. **107**, 026102 (2011).

[42] J. P. Perdew, K. Burke, and M. Ernzerhof, Phys. Rev. Lett. **77**, 3865 (1996).

[43] G. Kresse and J. Furthmüller, Phys. Rev. B **54**, 11169 (1996).

[44] J. Matthews, *Epitaxial Growth* (Academic, New York, 1975).

[45] A. F. Wright, J. Appl. Phys. **82**, 2833 (1997).

[46] A. U. Sheleg and V. A. Savastenko, Inorg. Mater. **15**, 1257 (1979).

[47] A. Polian, M. Grimsditch, and I. Grzegory, J. Appl. Phys. **79**, 3343 (1996).

[48] K. Tsubouchi, K. Sugai, and N. Mikoshiba, in *Ultrasonics Symposium*, edited by B. R. McAvoy (IEEE, New York, 1981), pp. 375–380.

[49] A. R. Smith, R. M. Feenstra, D. W. Greve, J. Neugebauer, and J. E. Northrup, Phys. Rev. Lett. **79**, 3934 (1997).

[50] A. R. Smith, R. M. Feenstra, D. W. Greve, M. S. Shin, M. Skowronski, J. Neugebauer, and J. E. Northrup, J. Vac. Sci. Technol. B **16**, 2242 (1998).

[51] J. E. Northrup, J. Neugebauer, R. M. Feenstra, and A. R. Smith, Phys. Rev. B **61**, 9932 (2000).

[52] D. Segev and C. G. Van de Walle, Surf. Sci. **601**, L15 (2007).

[53] J. E. Northrup, R. DiFelice, and J. Neugebauer, Phys. Rev. B **55**, 13878 (1997).

[54]C. D. Lee, Y. Dong, R. M. Feenstra, J. E. Northrup, and J. Neugebauer, Phys. Rev. B **68**, 205317 (2003).
[55]M. S. Miao, A. Janotti, and C. G. Van de Walle, Phys. Rev. B **80**, 155319 (2009).
[56]A. A. Baski, S. C. Erwin, and L. J. Whitman, Surf. Sci. **423**, L265 (1999).
[57]T. M. Jung, S. M. Prokes, and R. Kaplan, J. Vac. Sci. Technol. A **12**, 1838 (1994).
[58]N. Chetty and R. M. Martin, Phys. Rev. B **45**, 6089 (1992).
[59]N. Moll, A. Kley, E. Pehlke, and M. Scheffler, Phys. Rev. B **54**, 8844 (1996).